

Full Length Research Paper

Purification of an industrial aluminum alloy by melt stirring during ohno continuous casting process

Simbarashe Fashu*, Li Jianguo and Hu Qiao Dan

School of Material Science and Engineering, Shanghai Jiao Tong University, Shanghai, Dongchuan Road 800, 200240, China.

Accepted 11 March, 2011

With the purpose of upgrading the purity of a dilute industrial aluminum alloy during ohno continuous casting (OCC) process through the use of forced melt stirring; the critical stirring intensity required under a casting speed of 2 mm/min was numerically determined. The determined critical stirring intensity induces convective velocity magnitudes into the melt which are effective in transporting solutes from the solute boundary layer into the bulk melt. It was found that, with adequate melt stirring, production of substantially long and high purity ingots during OCC is possible before their purity diminishes to lower than the initial alloy purity.

Key words: Segregation, impurities, purification, stirring.

INTRODUCTION

The mode of redistribution of excess solutes accumulating at the solid-liquid interface during ohno continuous casting (OCC) is a key factor determining the final purity of the produced ingots (Hashimoto et al., 1995). In absence of adequate melt convection, the rejected solutes forms a thick enriched solute boundary layer at the solid-liquid interface upon which solute transport is solely through diffusion (Wanqi, 2001). Thus, purification of the ingot occurs only during the transient stage before the accretion of the solute boundary layer at the stationary solid-liquid interface and after that, the solid will maintain the initial composition of the alloy due to a high solute concentration in the liquid at the interface (Tiller et al., 1995). In order to obtain high purity ingots during OCC process, a sufficiently strong convection towards the solidification front, reduces the thickness of the boundary layer (Willers et al., 2008), thus lowering the solute concentration in the solid. Purification of metals during solidification by taking advantage of segregation and melt convection is now an established process and is more effective if the partition coefficients of solutes are

much less than unity. Mullin and Hulme (1958) equipped the zone refining process with an alternating magnetic field and obtained an enhanced purification rate in zone refining of semiconductors due to forced melt mixing. The emphasis of this article is placed upon using computer simulation to determine the adequate mechanical critical melt stirring intensity, required under a casting speed of 2 mm/min during OCC of aluminum rods to produce ingots of high purity. The lower casting speed (solidification rate) is used to increase the size of the mushy zone and the time for the solute rich liquid in the mushy zone to flow.

OCC process

Ohno continuous casting (OCC) process is a recently developed heated mold unidirectional continuous casting process used for producing superior, unidirectional rods and wires of substantial length (Ohno, 1986). The process is reliable in producing high purity wires and rods required mostly for the telecommunications industry and modern science technology, for example, video and audio cables (Motoyasu *et al.*, 1995). As shown schematically in Figure 1, the OCC process involves the continuous introduction of molten metal into an externally heated mould which is held slightly above the melting

*Corresponding author. E-mail: sfashu04@gmail.com. Tel/Fax: 0086-21-5474 4119.

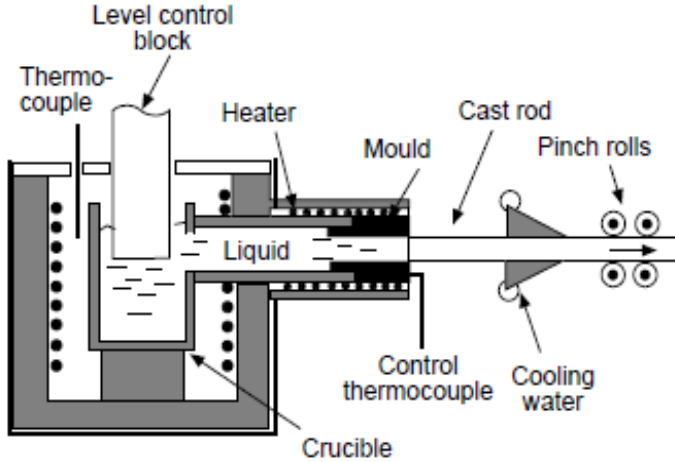


Figure 1. Schematic diagram of the horizontal OCC process.

point of the metal being cast; heat is extracted from the cast product by means of a cooling device located some distance from the mould exit. The solidified ingot is pulled with the pinch rollers placed some distance from the water cooling region.

MATHEMATICAL MODEL

Mechanical stirring OCC configuration

The OCC domain considered in our simulation is shown in Figure 2 and the regions of interest are the liquid in the heated mold and solid ingot, surrounding the solid-liquid interface where solidification and mass transfer occurs. Melt stirring was induced into the melt through mechanical rotation of a stirrer positioned at 30 mm from the mold exit as shown in Figure 3 to produce an effective axial flow field required for solute transport.

Governing equations

A macro-transfer model, based on the continuum model of Bennon and Incropera (1987), and reassessed by Prescott and Incropera (1987), was used for predicting the solute distribution during OCC of a multicomponent aluminum alloy.

Assumptions

1. All of the properties of the mixture can be obtained from the properties of its components in each phase.
2. All transport properties of each phase, such as thermal and electrical conductivity or viscosity, are constants.
3. The density is constant in each phase and the densities of the two phases are similar.
4. The mushy region is modeled by means of using the mixture viscosity.
5. Local equilibrium is assumed to exist at the solid-liquid interface, that is, the phase diagram is applied; $C_{i,s} = K_i C_{i,l}$.
6. The flow of the liquid phase is assumed to be incompressible, laminar and Newtonian.

7. Solutes diffusion coefficients are anisotropic and constant in each phase.

Based on the afore mentioned assumptions, the set of governing equations of heat, momentum and solute transport are:

Mass conservation equation:

$$\frac{\partial \rho}{\partial t} + \nabla \cdot (\rho \vec{u}) = 0 \quad (1)$$

Where t is the time, ρ is the density, \vec{u} is the average velocity of the mixture, which can be defined as $\vec{u} = f_s \vec{u}_s + f_l \vec{u}_l$, f_s and f_l are solid and liquid fractions, respectively.

Momentum conservation equation:

$$\frac{\partial (\rho \vec{u})}{\partial t} + \nabla \cdot (\rho \vec{u} \vec{u}) = -\nabla p + \nabla \cdot (\mu_l \nabla \vec{u}) - \frac{(1-f_l)^2}{(f_l + \epsilon)^3} (\vec{u} - \vec{u}_s) A_{mush} + S_m \quad (2)$$

where p is the pressure, μ_l is the dynamic viscosity of the melt, K is the permeability constant of the mushy zone, ϵ is a small number (0.001) to prevent division by zero, u_s is the solid velocity due to ingot pulling from the mushy zone, S_m is the momentum source which in our simulation is only due to mechanical stirring.

The enthalpy-porosity technique was used to treat the mushy zone as a pseudo porous medium, with the porosity of each cell being set to its liquid fraction. The variation of permeability is approximated as function of liquid mass fraction f_l using the Carman-Kozeny relation:

$$K = K_0 \frac{f_l^3}{(1-f_l)^2} \quad (3)$$

Where K_0 is a permeability constant depending on the morphology of the two-phase mushy region. $A_{mush} = \frac{\mu_l}{K_0}$ is the mushy zone constant and depends on the material. The value of K_0 is usually approximated as $K_0 = \frac{d^2}{180}$, where d denotes the dendrite arm spacing.

Energy conservation equation:

$$\frac{\partial (\rho H)}{\partial t} + \nabla \cdot (\rho H \vec{u}) = \nabla \cdot (k \nabla T) + S_h \quad (4)$$

Where H is the enthalpy, k is the thermal conductivity; T is the temperature and S_h the source term, is written as:

$$S_h = -\nabla \cdot [\rho (H_l - H) (\vec{u} - \vec{u}_s)]$$

The first term on the right hand side of Equation 4 represent the net

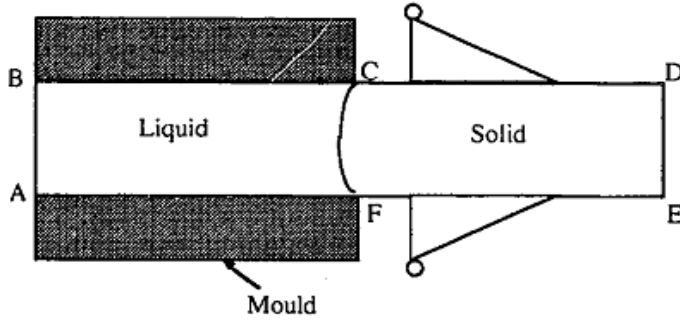


Figure 2. OCC domain considered in simulation.

Fourier diffusion flux. The enthalpy was computed as the sum of the sensible enthalpy, h , and the latent heat, ΔH :

$$H = h + \Delta H \quad (5)$$

Where:

$$h = h_{ref} + \int_{T_{ref}}^T C_p dT \quad (6)$$

Where h_{ref} = reference enthalpy, T_{ref} = reference temperature, C_p = specific heat at constant pressure. The latent heat content written in terms of the latent heat of the material, L is:

$$\Delta H = f_l L \quad (7)$$

The latent heat content varies between zero (for a solid) and L (for a liquid) and f_l is obtained from Equation 8. The liquid fraction is assumed to be linearly (Lever rule) proportional to temperature as:

$$f_l = \begin{cases} 1 & \text{when } T \geq T_l \\ \frac{T - T_s}{T_l - T_s} & \text{when } T_l \geq T \geq T_s \\ 0 & \text{when } T \leq T_s \end{cases} \quad (8)$$

Assuming that the solidus and liquidus lines are straight lines, the solidus and liquidus temperatures of solutes mixture are expressed as:

$$T_l = T_{melt} + \sum_{i=1}^n m_i C_i \quad (9)$$

$$T_s = T_{melt} + \sum_{i=1}^n \frac{m_i C_i}{k_i} \quad (10)$$

Where T_m is the fusion temperature, m_i is the slope of the liquidus line of binary phase diagram of solute i and aluminum and k_i is the partition coefficient of solute i in aluminum.

The solution for temperature is an iteration between the energy of Equation 4 and the liquid fraction of Equation 7, using the method

suggested by Voller and Swaminathan (1991) to update the liquid fraction.

Solute conservation equation:

$$\frac{\partial(\rho C_i)}{\partial t} + \nabla \cdot (\rho f_l \vec{u}_l C_{i,l} + (1-f_l) \vec{u}_s C_{i,s}) = \nabla \cdot [\rho f_l D_{l,m} \nabla C_{i,l} + (1-f_l) \rho D_{l,m,s} \nabla C_{i,s}] + S_c \quad (11)$$

Where, C_i is the total mass fraction of species i , $C_i = f_s C_s^i + f_l C_l^i$, D is the solute mass diffusion coefficient,

$S_c = -\nabla \cdot [\rho(C_l^i - C_i)(\vec{u} - \vec{u}_s)]$ is the advection source term in the mushy zone due to the relative phase motion. The subscripts l, l, c, m and s represents the species number, liquid, casting, mixture and solid respectively. The term on the right hand side of Equation 11 represents the net Fickian diffusion flux of solutes associated with the solid and liquid phases. The liquid velocity, u_l is found from the average velocity as follows:

$$\vec{u}_l = \frac{(\vec{u} - \vec{u}_s f_s)}{f_l} \quad (12)$$

The mixture quantities are defined in the following manner:

$$f_l + f_s = 1, \quad H = H_l f_l + H_s f_s, \quad D = D_l f_l + D_s f_s, \quad k = k_l f_l + k_s f_s$$

The energy and species conservation equations are closed, using the equilibrium phase diagram and the liquid fraction in the whole domain, f_l - T relationship is defined by the Lever rule as shown in Equation 7. The assumption of local equilibrium at the interface does not preclude the existence of non-equilibrium conditions on a macroscopic scale, which are considered in the macroscopic Equation 9.

Numerical solution

The generalized format of the governing equations contains the transient terms, convective terms, diffusion terms and source terms, hence, the numerical procedure of solving them only requires slight modifications for the format of source terms as suggested by Patankar (1980). The solidification model was introduced and iteratively solved in CFD Fluent 6.3.26 software with the aid of User Defined Subroutines and convenient source terms of governing equations were introduced through User Defined Functions (UDFs). A fully implicit control volume based formulation was used for the time dependent terms, and the combined convection/diffusion coefficients were discretized using an upwind scheme. In order to resolve the pressure-velocity coupling in the momentum equations, the SIMPLE algorithm was used and pressure was discretized by the PRESTO! method. A momentum source term due to mechanical stirring was introduced into the melt through Multiple Reference Frame (MRF) model. A full, two dimensional single domain, fixed uniform grid of Figure 2 was used for the numerical calculation. Because of the high nonlinearity and full coupled nature of the governing equations, under-relaxation factors were reduced accordingly to obtain converged solutions. Double-diffusive convection in the melt was intentionally neglected in order to test theoretical models for diffusive regime and compare them with simulation results of solute redistribution in absence of melt

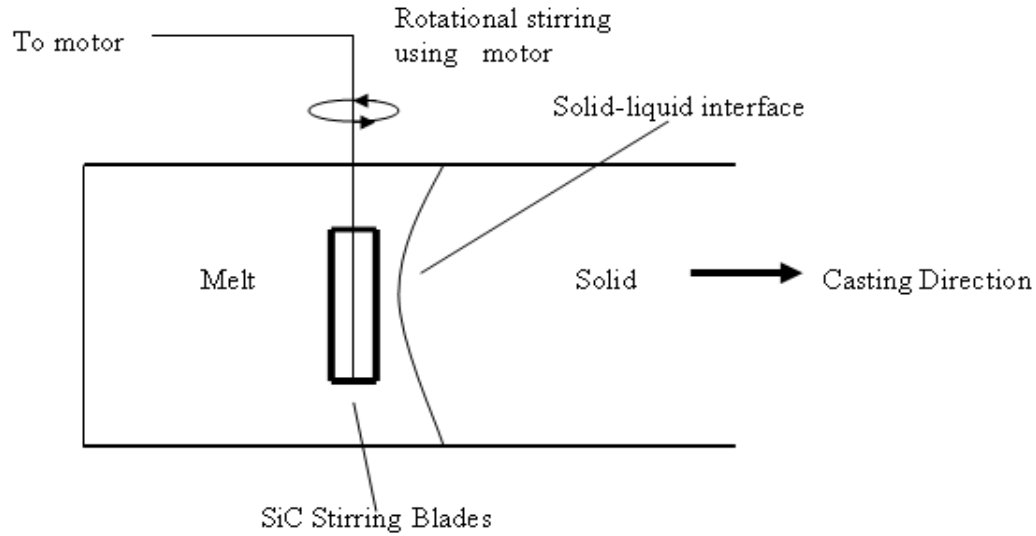


Figure 3. Positioning of a stirring blade in the melt near the interface for stirring.

Table 1. Thermo physical properties of Al 0.12wt%Cu 0.11wt%Si alloy.

Property	Units	Va values
Density of liquid /solid	kg/m ³	2400/2600
Specific heat	J/kgK	1080
Thermal conductivity of liquid	w/mK	90
Thermal conductivity of solid	w/mK	180
Diffusion coefficient of Cu in liquid	m ² /s	6e-9
Diffusion coefficient of Si in liquid	m ² /s	4e-9
Diffusion coefficient of Cu in solid	m ² /s	5e-13
Diffusion coefficient of Si in solid	m ² /s	3e-13
Partition coefficient of Si/Cu in Al	-	0.13/0.14
Melting temperature of Al	K	933
Slope of liquidus line Al-Cu/Al-Si	-	-3.43/-6
Viscosity of melt	Pa*s	0.0013
Melting heat	kJ	390

Table 2. Initial and boundary conditions.

Property	Units	Value
Melt inlet temperature	K	938
Melt inlet velocity	mm/min	2
Ingot pulling speed	mm/min	2
Heat transfer coefficient of Al in air	w/m ² K	414
Heat transfer coefficient of Al in water spray	w/m ² K	10000-50000
Temperature of heated mold	K	938

convection. Furthermore, the alloy is dilute, such that, solutal diffusion is negligible, and the use of a heated mold in horizontal OCC with gravity vector being perpendicular to thermal gradient

makes thermal convection effects to be insignificant (Verhoeven, 1968).

The industrial aluminum alloy under consideration is composed of copper and silicon as major impurities. Thermo-physical properties of the industrial dilute aluminum alloy and the initial and boundary conditions used in this simulation are shown in Tables 1 and 2, respectively. The solid-liquid interface position was controlled to be just near the stirring blade through adjustment of cooling in the water spray region.

SIMULATION RESULTS AND DISCUSSION

Validation of solidification results with published literature

In order to validate the solidification model which was used in our computations, the model was compared against theory and experimental results from literature. Lee et al. (2004) used Bridgman growth to grow ingots of 0.4 and 5.5 mm diameter in absence of external melt convection using Al-4%wtCu at a casting speed of 0.4 $\mu\text{m/s}$ and produced 40 mm ingots during transient state before the solute boundary layer had sufficient time to build. The Electron Microprobe Analysis (EMPA) composition profile of short solid samples and liquid was done as shown in Figure 4.

Simulation to show the capability of the solidification model was done using the same conditions as those used by Lee et al. (2004). Figure 5 shows the simulated copper solute redistribution after OCC of 5.5 mm ingots during the transient state. This result is in good agreement with experimental results obtained by Lee et al. (2004) as shown in Figure 4, showing that the model is capable of computing solute redistribution at the casting speeds considered.

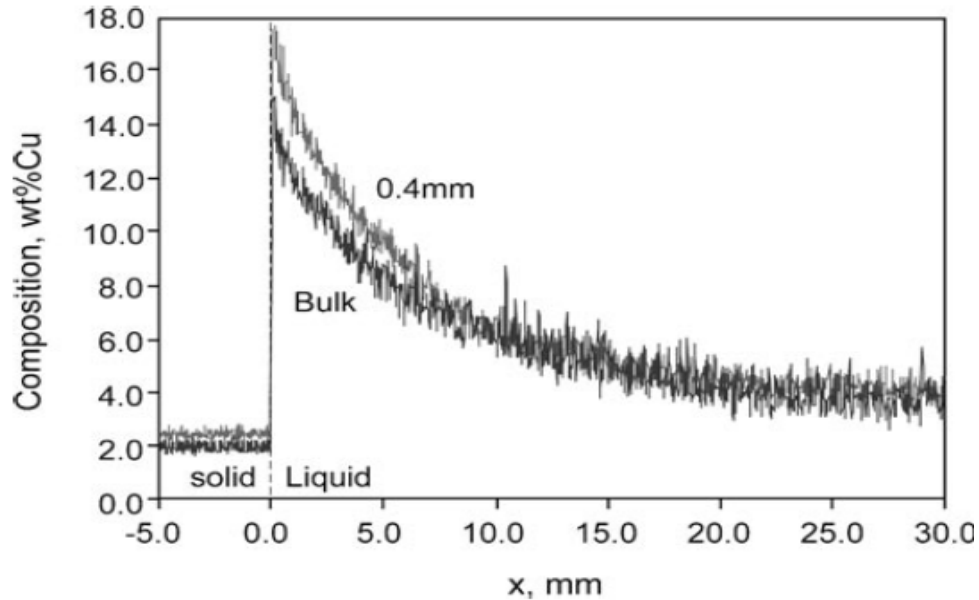


Figure 4. Line scan EPMA result of the composition profiles in 0.4 and 5.5 mm (bulk) diameter and 40 mm long ingots of Al-4%wtCu alloy unidirectionally solidified with Bridgman furnace at $0.4 \mu\text{m/s}$ (Lee et al., 2004).

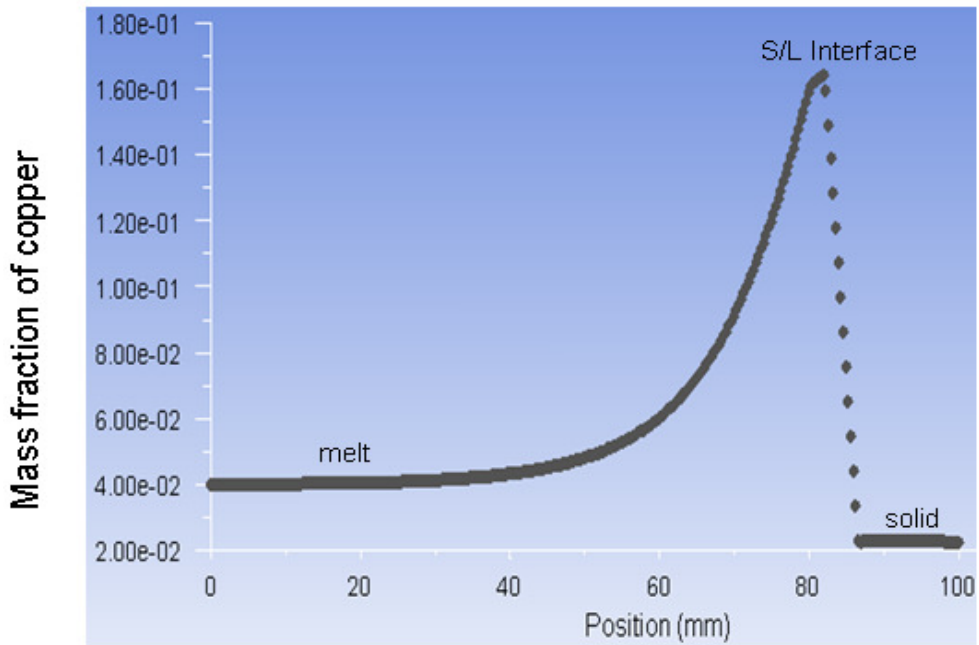


Figure 5. Solute redistribution obtained by simulation using experimental conditions from Lee et al. (2004).

Solidification and mechanical stirring results

Figure 6 shows the temperature distribution profile during steady OCC process. The solidus and liquidus fronts are stationary and solidification starts at the centre of the ingot, thus avoiding casting defects. Figure 7 shows the

aluminum redistribution after the OCC process has reached steady state in composition when there is no fluid flow and the solute distribution is caused only by the diffusion mechanism. This is in agreement with theory of Tiller et al. (1995), which states that the solute redistribution is constant, once steady state condition is

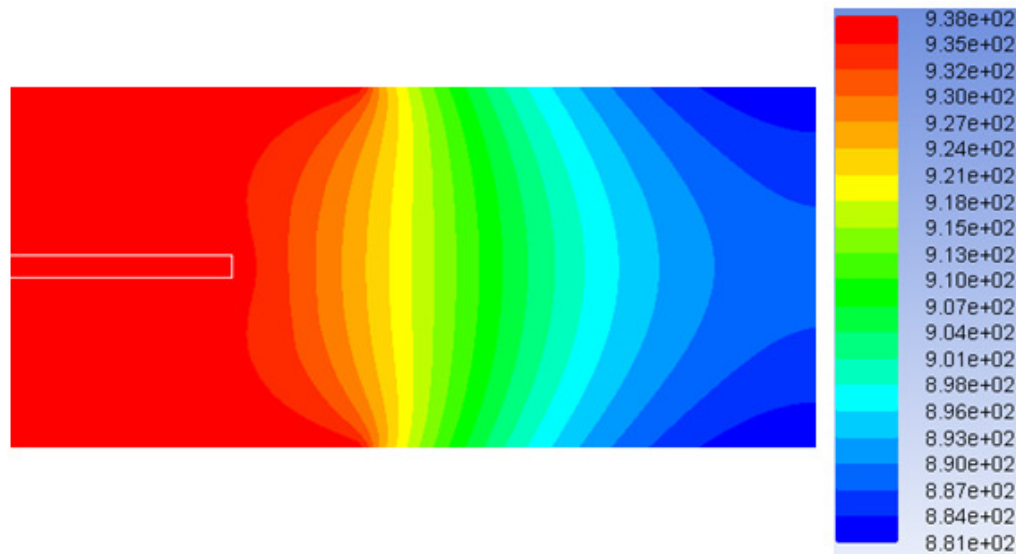


Figure 6. Temperature distribution profile.

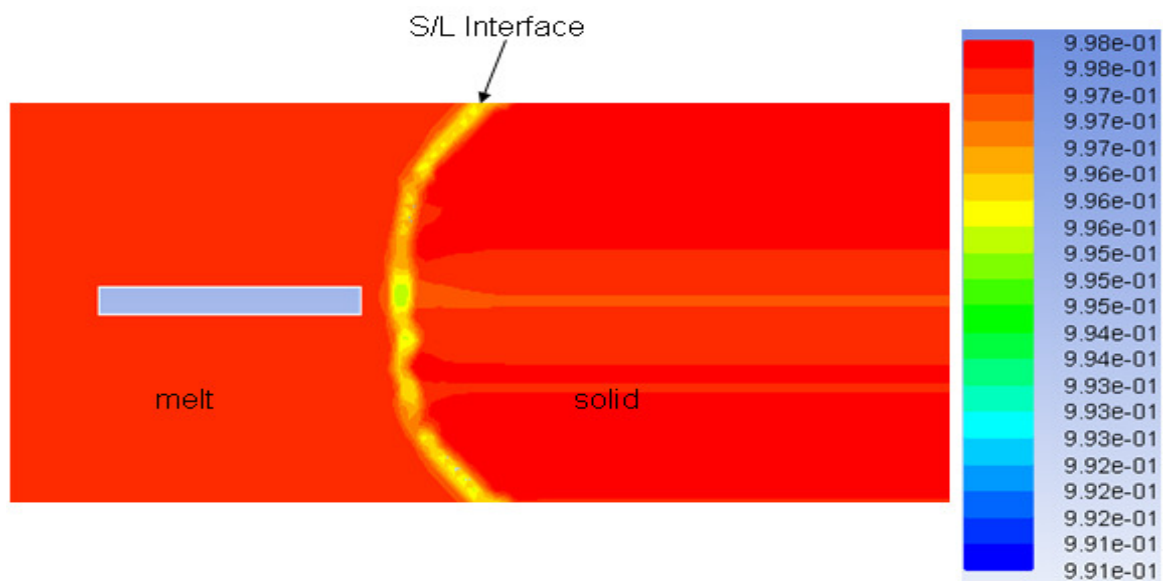


Figure 7. Aluminum redistribution at steady state in absence of melt stirring.

attained. Figure 8 shows the corresponding axial aluminum redistribution near the center of the ingot. Purification of the ingot occurs slightly during the transient process before the solute boundary layer is established. Using unsteady state simulation, it was found that about 500 mm ingots were cast to reach that state in composition. After attaining steady state composition, the accumulated solutes prevent solute redistribution and the solute concentration in the entire casting remains equal to the initial value and remains constant during OCC process because solute diffusion is a very slow process.

Thus, the solute diffusion coefficient, D_i , of the macroscopic solute transport in Equation 11 will be almost zero, and although the solute will be microscopically rejected at the solid-liquid interface, there will be no mechanism to transport the solute. This same solute redistribution behavior was also shown by Diao and Tsai (1993) during directional solidification of an Al-4.1%wtCu alloy in absence of melt convection. The critical stirring intensity required to produce ingots of highest purity during OCC process was obtained from rigorous trial and error using different stirring rates. Figures 9 and 10 show the solute distribution in ingot and

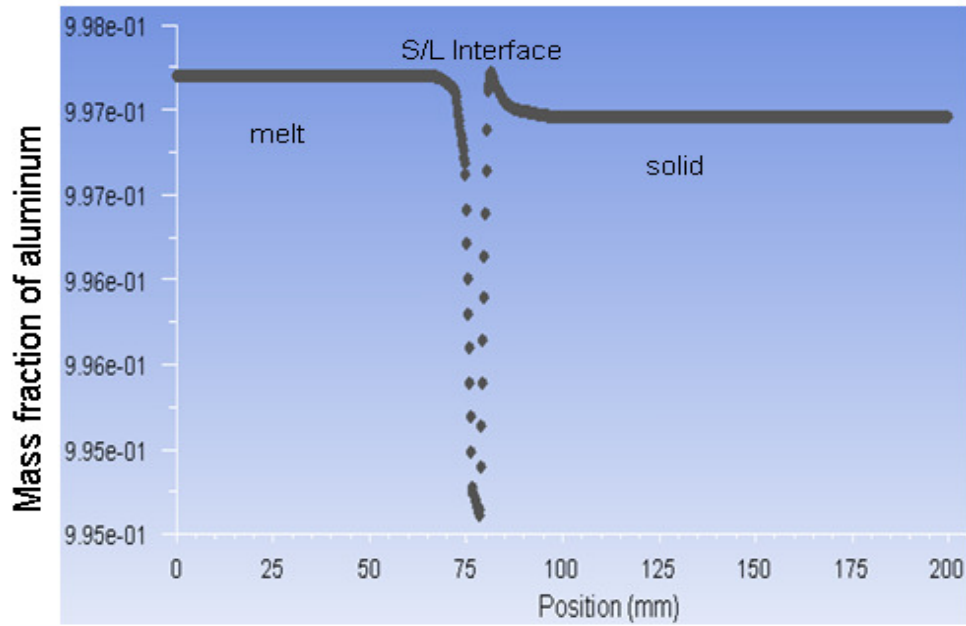


Figure 8. Axial distribution of aluminum in absence of melt stirring.

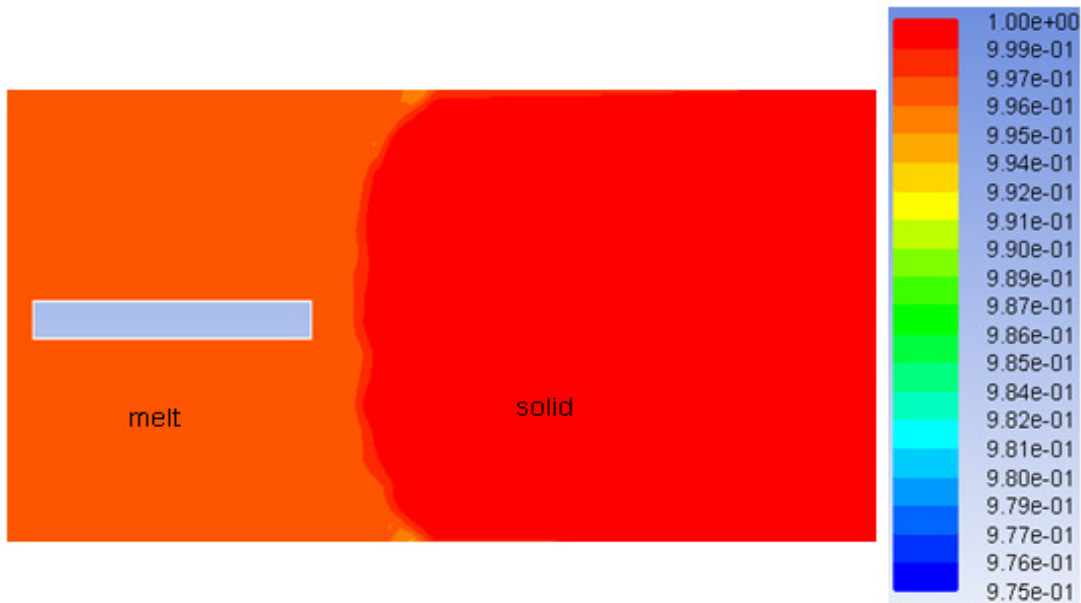


Figure 9. Aluminum redistribution in presence of optimum melt stirring of 10 rpm, after casting 2 m ingot.

its corresponding axial distribution, in presence of optimum stirring intensity, (Figure 11) for casting of 2 m ingot. Stirring significantly increased the ingot purity level from 99.77 to above 99.925%Al at the center of the ingot where stirring is more effective. The sides of the ingots are a bit less pure due to the poor design of the stirrer used. Since the fresh melt will continuously move into the heated mold during OCC process, it will dilute the bulk melt and maintain it at a low solute composition for a long

time. When the solute level of the ingots becomes higher than the initial alloy being used, then the process should be stopped and the melt discarded for other uses.

Conclusions

The critical stirring intensity required under an optimum casting speed to produce aluminum ingots of high purity

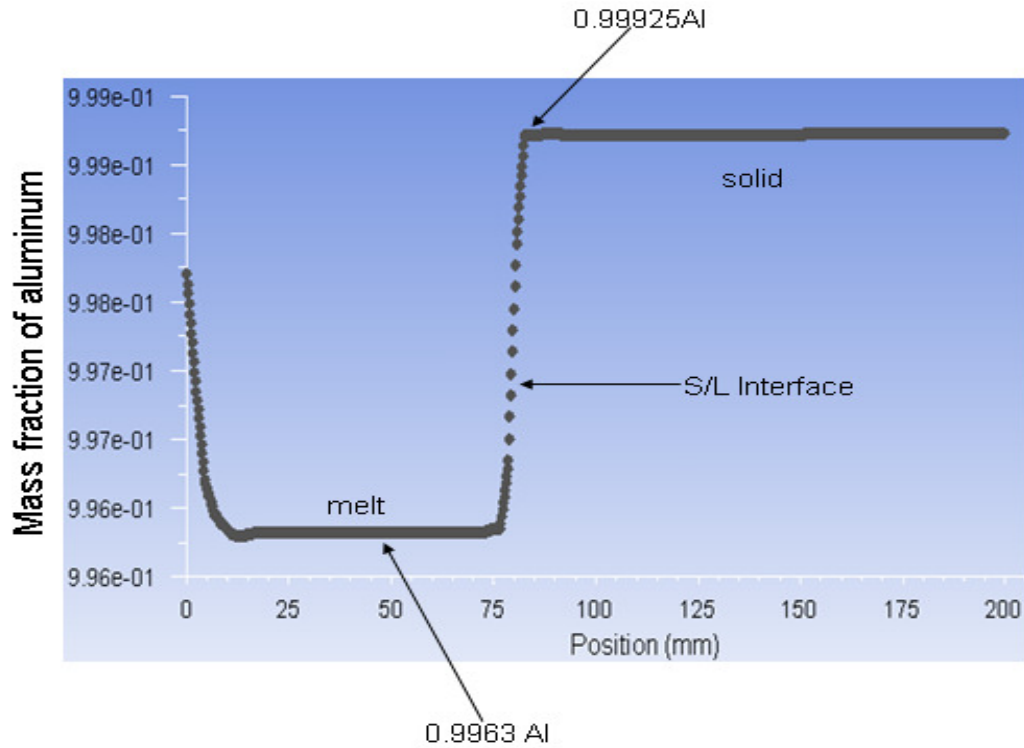


Figure 10. Axial aluminum redistribution at in presence of optimum melt stirring of 10 rpm, after casting 2 m ingot.

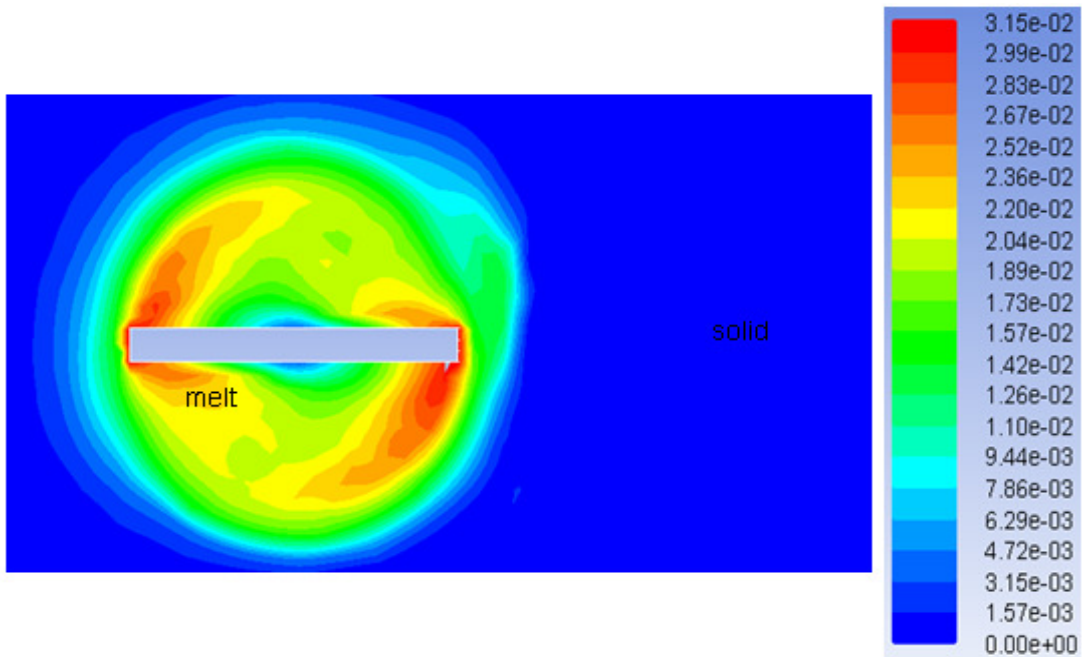


Figure 11. Velocity profile in m/s for optimum mechanical melt stirring of 10 rpm.

during OCC was determined by numerical simulation. This was done through melt stirring near the phase change region to produce a special axial rotating melt

flow field of adequate magnitude and direction. The industrial aluminum alloy is very dilute, and continuous flow into the heated mold makes it possible to produce

long and pure ingots before their purity level falls below the initial alloy composition. Thus, with optimization of casting speed and stirring intensity, high purity ingots at high production rates are possible to achieve during OCC process. This, of course should be accomplished with a good stirrer design, effective in mechanically stirring near the whole interface region.

ACKNOWLEDGEMENTS

This work was supported by the National Natural Science Foundation of China (50804030), China Post-Doctoral Science Foundation through the First Class Funding (20080430084) and the Special Funding (200902230) programs, and Shanghai Post-Doctoral Scientific Program (08R214135). We also acknowledge Instrumental Analysis Centre, SJTU for help in microstructure characterization. Thanks to Professor Lu Hao, for helpful discussion, and provision of CFD Fluent 6.3.26 Software.

REFERENCES

- Bennon WD, Incropera FP (1987). Continuum model for momentum, heat and species transport in binary solid-liquid phase change systems – I. *J. Heat Mass Transf.*, 30(20): 2166-2170.
- Diao QZ, Tsai HL (1993). Modeling of solute redistribution in the mushy zone during solidification of aluminum-copper alloys. *Metall. Trans.*, 24A: 963-973.
- Hashimoto E, Ueda Y, Kondo T (1995). Purification of Ultra-High Purity Aluminum. *J. Phys.*, 5: 153-157.
- Lee JH, Shan L, Miyahara H, Trivedi R (2004). Diffusion coefficient measurement in liquid metallic alloys. *Metall. Trans.*, 35B: 909-917.
- Motoyasu G, Soda H, McLean A, Wang Z (1995). Pilot scale casting of single crystals copper wires by the Ohno Continuous Casting Process. *J. Mater. Sci.*, 30(21): 5438-5448.
- Mullin JB, Hulme KF (1958). The use of electromagnetic stirring in zone refining. *J. Electron. Control.*, 14: 170-174.
- Ohno A (1986). Continuous casting of single crystal ingot by the OCC process. *J. Metals.*, 38: 14-16.
- Patankar SV (1980). *Numerical Heat Transfer and Fluid Flow*. Hemisphere, Washington DC, Hemisphere Publishing Corporation, pp. 126-134.
- Prescott PJ, Incropera FP (1991). Modeling of dendritic solidification systems: Reassessment of the continuum momentum equation. *Int. J. Heat Mass Transf.*, 34: 2351–2359.
- Tiller WA, Jackson KA, Rutter JW, Chalmers B. (1953). The redistribution of solute atoms during the solidification of metals. *Acta Metall.*, 1: 428-437.
- Verhoeven JD. (1968). The growth of off-eutectic composites from stirred melts. *Trans., AIME*, 242: 1937-1942.
- Voller VR, Swaminathan CR. (1991). General source-based method for solidification phase change. *Numer. Heat Transf.*, 19B(2): 175-189.
- Wanqi J (2001). Solute redistribution and segregation in solidification processes. *Sci. Technol. Adv. Mater.*, 2: 29-35.
- Willers B, Eckert S, Nikrityuk PA, Rübiger D, Dong J, Eckert K, Gerberth G. (2008). Efficient melt stirring using pulse sequences of a rotating magnetic field Part II. *Metall. Met. Transf.*, 39B: 304-316.